

Theoretical study of the aluminum melting curve to very high pressure

John A. Moriarty, David A. Young, and Marvin Ross

Lawrence Livermore National Laboratory, University of California, Livermore, California 94550

(Received 22 November 1983)

A detailed theoretical study of the Al melting curve from normal melting conditions to pressures in the vicinity of 2 Mbar is presented. The analysis is based on two parallel, but distinct, treatments of the metal: the first from rigorous generalized pseudopotential theory involving first-principles nonlocal pseudopotentials and the second from a parametrized local pseudopotential model which has been accurately fit to first-principles band-theory and experimental equation-of-state data. Both treatments utilize full lattice-dynamical calculations of the phonon free energy in the solid, within the harmonic approximation, and fluid variational theory to obtain the free energy of the liquid. Particular attention is focused on the choice of the reference system in implementing the fluid variational theory. It is shown that in Al the soft-sphere model of Ross produces a lower (and hence more accurate) liquid free energy than either the hard-sphere or one-component-plasma reference systems, and is, moreover, necessary to obtain a reasonable quantitative description of the melting properties. With the soft-sphere system, the two theoretical treatments give results in good overall agreement with each other and with experiment. In particular, melting on the shock Hugoniot is predicted to begin at about 1.2 Mbar and to end at about 1.55 Mbar, in excellent agreement with the recent preliminary measurements of McQueen.

I. INTRODUCTION

The calculation of the melting curve in metals remains a challenging and important theoretical problem, with the basic difficulty being that of obtaining free-energy differences between solid and liquid phases which are only a tiny fraction of the cohesive energy. For simple metals, the basic ingredients required for a quantitative theory of melting were identified some time ago by Stroud and Ashcroft.¹ These ingredients include pseudopotential perturbation theory^{2,3} for treating the ion-electron interaction in both the solid and liquid phases, a lattice-dynamics model for the phonon free energy of the solid, and fluid variational theory⁴ for calculating the free energy of the liquid. Using a simple one-parameter local pseudopotential, a self-consistent Debye model for the phonons, and a hard-sphere reference fluid for the liquid, Stroud and Ashcroft were able to obtain a reasonable quantitative description of the melting curve in Na to 40 kbar. Good results for the zero-pressure melting properties of Li, Na, K, and Al were subsequently obtained by Jones⁵ with a similar method. This success, while encouraging, appears in retrospect to be somewhat fortuitous, however. Recent work on the alkali metals Li, Na, and K by Young and Ross,⁶ for example, shows that the melting curve depends significantly on the details of the calculation and in particular on the choice of reference system in the fluid variational theory. These authors found the hard-sphere reference fluid to be qualitatively inadequate once the simple Debye model was replaced by a full lattice-dynamical calculation of the phonon spectrum. Thus even for simple metals, an unambiguous universal procedure for calculation of the melting curve is not yet at hand.

The present paper contains an in-depth analysis of the

melting properties of another prototype simple metal, aluminum, both near normal density and also under high pressure. Previous related theoretical work on melting in this metal consists only of the early calculations of the latent heat of fusion by Hartmann⁷ and of the zero-pressure melting properties by Jones.⁵ The present work goes beyond these treatments in several important ways:

(i) We investigate for the first time the importance of the choice of the pseudopotential itself to the result by considering parallel calculations of the melting curve with both a parametrized local pseudopotential and a rigorous nonlocal pseudopotential obtained from first principles. For the former we adopt the two-parameter Harrison local pseudopotential model² used by Jones (herein denoted as the HLP model), and for the latter that given by the generalized pseudopotential theory (GPT) of the present first author.⁸ Our GPT result, we believe, represents the only entirely first-principles calculation of a melting curve yet obtained. Moreover, extensive comparisons with recent nonperturbative band-theory calculations in the solid⁹ demonstrates that the GPT is capable of giving accurate structural energy differences in Al on the scale required in the melting problem.

(ii) As done by Young and Ross on the alkali metals,⁶ our treatment of the phonon free energy is based on a full lattice-dynamical calculation of the vibrational spectrum in the solid using the specified pseudopotentials within the harmonic approximation. The neglect of anharmonic contributions to the free energy is partially justified by the work of Stroud and Ashcroft,¹ who found only a weak temperature dependence in their calculated Debye temperature, especially under compression, and also by recent molecular-dynamics studies on Na,¹⁰ where it was found that the anharmonic free energy was indeed small (less than 10% of the heat of fusion at melting). Moreover, al-

though model studies of anharmonicity¹¹ using various approximation methods (perturbation theory, self-consistent phonons, cell models) suggest significant corrections to high-temperature thermodynamics properties in general, the molecular-dynamics results show explicitly that near melting the anharmonic free energy can be overestimated by as much as an order of magnitude with the use of such methods. Anharmonic contributions to the melting properties of Al may not be completely negligible, but, on the other hand, their effect is probably small, particularly at high pressure, relative to other uncertainties in the calculation.

(iii) We make a full investigation of the choice of fluid reference system using the rigorous GPT pseudopotentials. For calculating the thermodynamic properties of simple-metal liquids, hard-sphere,⁴ soft-sphere,^{12,13} and one-component-plasma^{13,14} reference systems have now been developed. In the case of Al, we find that the soft-sphere model of Ross¹² is optimum in the sense of producing the lowest overall Helmholtz free energy at all volumes and temperatures of interest in melting. Use of the soft-sphere reference system is also found necessary to obtain a quantitatively reasonable description of the melting curve in both the GPT and HLP treatments.

(iv) The final significant new feature of our work is that the melting curves have been extended into the very-high-pressure regime (up to 2 Mbar). This is of considerable current interest in Al, because this metal is being used as a high-pressure equation-of-state (EOS) standard. In addition, it is now possible to detect melting on the shock Hugoniot of metals through the measured sound speed,¹⁵ and there has been a very recent experimental study of this effect in Al.¹⁶ We present here a prediction of where this melting should occur based on our HLP model. The same model has also been used to investigate a number of other thermodynamic properties of Al, as will be reported separately.

In Sec. II we summarize the elements of pseudopotential theory which are relevant to the melting problem and also discuss our two choices of pseudopotential. In Sec. III we review the statistical-mechanical models used in the present analysis to obtain the free energies in both the solid and liquid phases of the metal. Then in Sec. IV our melting results on Al are presented and discussed. We conclude in Sec. V.

II. PSEUDOPOTENTIAL THEORY

A. General expressions

The elements of pseudopotential theory that we require are discussed at length in Refs. 2, 3, and 8. In brief, the electron-ion interaction in a simple metal may be rigorously represented by a nonlocal pseudopotential (operator) of the form

$$w(\vec{r}, \vec{r}') = \left[-\frac{Ze^2}{r} + v_{\text{scr}}(r) + v_{\text{oh}}(r) \right] \times \delta(\vec{r} - \vec{r}') + w_{\text{core}}(\vec{r}, \vec{r}'), \quad (1)$$

where Z is the valence of the metal ($Z=3$ for Al), v_{scr} and v_{oh} are the potentials arising from the electron screening and orthogonalization-hole densities, n_{scr} and n_{oh} , respectively, and w_{core} is the (repulsive) core pseudopotential. The corresponding form-factor coupling plane waves $\langle \vec{k} + \vec{q} |$ and $| \vec{k} \rangle$ on the constant-energy surface $\epsilon_{\vec{k}} = \hbar^2 k^2 / 2m$ is then

$$w(\vec{k}, \vec{q}) \equiv \langle \vec{k} + \vec{q} | w | \vec{k} \rangle = -\frac{4\pi Ze^2}{q^2 \Omega} + v_{\text{scr}}(q) + v_{\text{oh}}(q) + w_{\text{core}}(\vec{k}, \vec{q}), \quad (2)$$

where Ω is the atomic volume of the metal. For a weak simple-metal pseudopotential, the screening potential $v_{\text{scr}}(q)$ may be obtained self-consistently by using first-order perturbation theory together with the exchange-correlation modified Poisson equation

$$v_{\text{scr}}(q) = \frac{4\pi e^2}{q^2} [1 - G(q)] n_{\text{scr}}(q), \quad (3)$$

where the exchange-correlation function $G(q)$ is that for the corresponding uniform electron gas.

The central theoretical quantity of interest to us is the total binding energy per atom of the valence electrons in the metal, E_{bind} , for an arbitrary static configuration of the ions. This may be obtained in second-order perturbation theory as a sum of a large volume term, E_{vol} , independent of the individual positions of the ions \vec{R}_i , and a much smaller structural energy, E_{struc} , both of which are functionals of the pseudopotential. Specifically, one can write

$$E_{\text{bind}} = E_{\text{vol}} + E_{\text{struc}}, \quad (4)$$

with

$$E_{\text{vol}} = \frac{3}{5} Z \epsilon_F + Z \epsilon_{\text{xc}} - \frac{9}{10} \frac{(Ze)^2}{R_a} + \frac{2\Omega}{(2\pi)^3} \int_{k < k_F} w_{\text{core}}(\vec{k}, \vec{0}) d\vec{k} + \dots, \quad (5)$$

where the ellipsis includes all second-order terms, and

$$E_{\text{struc}} = E_{\text{es}}(Z^* e) + \frac{9}{10} \frac{(Z^* e)^2}{R_a} + \sum'_{\vec{q}} |S(\vec{q})|^2 F(q). \quad (6)$$

In Eq. (5), the first two terms are, respectively, the kinetic energy and exchange-correlation energy of the uniform electron gas with Fermi energy $\epsilon_F = \hbar^2 k_F^2 / 2m$, while in the third term R_a is the atomic-sphere radius ($\Omega = 4\pi R_a^3 / 3$). Explicit expressions for the second-order terms in that equation can be found in Ref. 8. In Eq. (6), Z^* is the effective valence

$$Z^* = Z - \int n_{\text{oh}}(r) d\vec{r}, \quad (7)$$

E_{es} is the electrostatic (or Madelung) energy of point charges $Z^* e$ embedded in a uniform compensating background, $S(\vec{q})$ is the structure factor

$$S(\vec{q}) = \frac{1}{N} \sum_{i=1}^N e^{-i\vec{q} \cdot \vec{R}_i}, \quad (8)$$

and $F(q)$ is the energy-wave-number characteristic,

$$F(q) = \frac{2\Omega}{(2\pi)^3} \int_{k < k_F} \frac{|w(\vec{k}, \vec{q})|^2}{\epsilon_{\vec{k}} - \epsilon_{\vec{k} + \vec{q}}} d\vec{k} - \frac{2\pi e^2 \Omega}{q^2} \{ [1 - G(q)][n_{\text{scr}}(q)]^2 + G(q)[n_{\text{oh}}(q)]^2 \}. \quad (9)$$

The quantities Z^* and $F(q)$ are characteristic functions of volume and all of the structure dependence in E_{bind} is contained in E_{es} and $S(\vec{q})$. Generally speaking, $Z^* > Z$ because n_{oh} represents a negative electron density, with Z^* increasing with decreasing volume. For Al in the GPT, Z^*/Z varies between about 1.05 and 1.15 over the volume range from 30% expansion to twofold compression.

B. GPT first-principles pseudopotential

In optimized form, the GPT nonlocal core pseudopotential for a simple metal can be written as

$$w_{\text{core}}(\vec{k}, \vec{q}) = v_{\text{core}}(q) + \sum_{\vec{c}} (\epsilon_{\vec{k}} - E_{\vec{c}}^{\text{vol}}) \langle \vec{k} + \vec{q} | \phi_{\vec{c}} \rangle \langle \phi_{\vec{c}} | \vec{k} \rangle, \quad (10)$$

where v_{core} is the full (one-site) core potential and $\phi_{\vec{c}}$ and $E_{\vec{c}}^{\text{vol}}$ are the corresponding core states and core energies in the metal at volume Ω . All of the ingredients in w_{core} may be calculated from first-principles considerations⁸ within the general theoretical framework of the Kohn-Sham density-functional formalism.¹⁷

In the case of Al, one may additionally account for the small perturbing effects of unoccupied d states above the Fermi level by adding appropriate hybridization terms to n_{oh} and w_{core} ,⁸ with Eqs. (1)–(9) above otherwise unchanged. This is the empty- d -band limit of the GPT. In the present context, these hybridization terms are of negligible importance near normal density, but they do grow slowly in magnitude under compression. In all of the GPT calculations described below, these terms have been retained for completeness.

One further variable aspect of the above formalism is the choice of exchange-correlation functions ϵ_{xc} and $G(q)$. The latter has the rigorous limits

$$G(q) = \begin{cases} -\frac{k_F^2}{4\pi e^2} \frac{d^2[n\epsilon_{\text{xc}}(n)]}{dn^2} (q/k_F)^2 & \text{as } q \rightarrow 0, \\ \xi(n) & \text{as } q \rightarrow \infty, \end{cases} \quad (11)$$

for electron density $n = Z/\Omega$, with $\xi(n)$ a density-dependent constant. The $q \rightarrow 0$ limit of Eq. (11) insures that the compressibility sum rule is exactly satisfied. Both $G(q)$ at intermediate q and $\xi(n)$, however, still remain to be firmly established.¹⁸ In the GPT we use the $G(q)$ calculated by Geldart and Taylor¹⁹ from electron-gas theory as an interpolation between the limits of Eq. (11) for any given form of ϵ_{xc} . For ϵ_{xc} we employ the exchange-correlation functional determined by Hedin and Lundqvist.²⁰

C. Harrison local pseudopotential (HLP)

The alternative to a rigorous calculation of w_{core} is to introduce a parametrized model potential for this quantity. If a fixed local potential is chosen, one has the immediate simplification

$$w_{\text{core}}(\vec{k}, \vec{q}) \rightarrow w_{\text{core}}(q), \quad (12)$$

so that all \vec{k} -space integrals, such as those in Eqs. (5) and (9), can be done analytically. In addition, the orthogonalization hole exactly vanishes,²

$$n_{\text{oh}} \rightarrow 0 \quad \text{and} \quad Z^* \rightarrow Z, \quad (13)$$

as do all of the second-order terms in E_{vol} . The total-binding-energy expression (4) then collapses to the simplified form

$$E_{\text{bind}} = \frac{3}{5} Z \epsilon_F + Z \epsilon_{\text{xc}} + Z w_{\text{core}}(0) + E_{\text{es}}(Ze) + \sum_{\vec{q}}' |S(\vec{q})|^2 F(q), \quad (14)$$

with

$$F(q) = -\frac{q^2 \Omega}{8\pi e^2} \left[-\frac{4\pi Z e^2}{q^2 \Omega} + w_{\text{core}}(q) \right]^2 \times \left[\frac{\epsilon^H(q) - 1}{\epsilon^H(q) - G(q)[\epsilon^H(q) - 1]} \right], \quad (15)$$

where $\epsilon^H(q)$ is the familiar Hartree or Lindhard dielectric function.

In the present work, we use a simple real-space core pseudopotential originally suggested by Harrison,²

$$w_{\text{core}}(r) = \frac{\beta}{8\pi r_c^3} e^{-r/r_c}, \quad (16)$$

which yields

$$w_{\text{core}}(q) = \frac{\beta}{\Omega} \frac{1}{[1 + (r_c q)^2]^2}, \quad (17)$$

where β and r_c are free parameters. In order to maximize our latitude in choosing these latter quantities, we have further parametrized the exchange-correlation function $G(q)$ in the form

$$G(q) = \alpha \xi \frac{q^2}{\alpha q^2 + \xi k_F^2} = \begin{cases} \alpha(q/k_F)^2 & \text{as } q \rightarrow 0, \\ \xi & \text{as } q \rightarrow \infty, \end{cases} \quad (18)$$

treating α and ξ as additional free parameters. The four quantities β , r_c , α , and ξ are then established by fitting to independent EOS data, as described in Sec. III C.

For calculating thermodynamic properties of metals, the two principal virtues of a parametrized local pseudopotential approach are (i) the volume dependence of E_{bind} remains analytic so that derivative quantities such as the pressure can be easily and accurately calculated, and (ii) one can incorporate desired experimental or theoretical data into the theory. With regard to the latter, one of our

primary motives in developing the HLP model has been to permit an accurate fit to nonperturbative first-principles energy-band calculations of the pressure at high compression. This compensates for the fact that the higher-order terms in E_{bind} have been explicitly dropped in the pseudopotential perturbation theory. At the same time, the neglect of nonlocality in the pseudopotential can be expected to significantly restrict its transferability from one physical property to another. In the present context, the central question in this regard is whether or not a local pseudopotential fit to largely volume-dependent properties (i.e., EOS data) can be reliably applied to calculate a largely structure-dependent property (i.e., the melting curve).

III. STATISTICAL MECHANICS

A. Solid phase

The Helmholtz free energy of the solid can be written as a sum of the static-lattice binding energy (i.e., $E_{\text{bind}}^{\text{sol}} \equiv E_{\text{bind}}$ evaluated for a particular crystal structure) and the phonon free energy of the ions:

$$\begin{aligned} A_{\text{sol}}(\Omega, T) &= E_{\text{bind}}^{\text{sol}}(\Omega) + A_{\text{ph}}(\Omega, T) \\ &= E_{\text{bind}}^{\text{sol}}(\Omega) + E_{\text{ph}}(\Omega, T) - TS_{\text{ph}}(\Omega, T), \end{aligned} \quad (19)$$

where E_{ph} and S_{ph} are the phonon total energy and entropy, respectively. For a perfectly periodic solid, the structure component of $E_{\text{bind}}^{\text{sol}}$ reduces to the simple form

$$E_{\text{struc}}^{\text{sol}}(\Omega) = \frac{1}{2} \frac{(Z^*e)^2}{R_a} (1.8 - \alpha_{\text{sol}}) + \sum'_{\vec{q}=\vec{K}} F(q), \quad (20)$$

and, in the harmonic-phonon approximation,

$$A_{\text{ph}}(\Omega, T) = (k_B T / N) \sum_{\vec{q}, \lambda} \ln \{ 2 \sinh [h \nu_{\lambda}(\vec{q}) / 2k_B T] \}. \quad (21)$$

In Eq. (20), α_{sol} is the geometric electrostatic constant for the crystal lattice in question and the sum over $F(q)$ includes only nonzero reciprocal-lattice vectors \vec{K} . For the fcc crystal structure of Al, $\alpha_{\text{sol}} = 1.79175$. The sum in Eq. (21) is over all phonon branches λ and wave vectors \vec{q} in the first Brillouin zone of the reciprocal lattice. The phonon frequencies $\nu_{\lambda}(\vec{q})$ themselves are calculated directly in terms of the characteristic functions Z^* and $F(q)$ by standard techniques^{2,3} and the Brillouin-zone sum then done numerically as a function of volume and temperature.^{6,21}

Structural phase stability in solid Al has recently been studied in great detail with the GPT.⁹ At zero temperature it is found that the observed fcc structure is stable from normal density until beyond twofold compression corresponding to a pressure range of ~ 3.6 Mbar. In addition, the bcc structure is found to be mechanically unstable in this regime, so that no temperature-induced transition to bcc prior to melt (as occurs, for example, in the alkali and alkaline-earth metals) is expected. We have assumed in our calculations, therefore, that Al melts out of the fcc structure everywhere along the melting curve.

B. Liquid phase

The corresponding Helmholtz free energy of the liquid is taken as

$$\begin{aligned} A_{\text{liq}}(\Omega, T) &= E_{\text{bind}}^{\text{liq}}(\Omega, T) + E_{\text{gas}}(T) \\ &\quad - T[S_{\text{exc}}(\Omega, T) + S_{\text{gas}}(\Omega, T)], \end{aligned} \quad (22)$$

where E_{gas} and S_{gas} are the kinetic energy and entropy of an ideal gas of atoms at temperature T :

$$E_{\text{gas}}(T) = \frac{3}{2} k_B T \quad (23)$$

and

$$S_{\text{gas}}(\Omega, T) = \frac{3}{2} k_B + k_B [\ln(\Omega/\Lambda^3) + 1], \quad (24)$$

with

$$\Lambda = \frac{h}{(2\pi M k_B T)^{1/2}}, \quad (25)$$

and M is the atomic mass. The quantities $E_{\text{bind}}^{\text{liq}}$ and S_{exc} are the total, configurationally averaged binding energy and excess entropy of the liquid, respectively. The structure component of $E_{\text{bind}}^{\text{liq}}$ can be written

$$\begin{aligned} E_{\text{struc}}^{\text{liq}}(\Omega, T) &= \frac{1}{2} \frac{(Z^*e)^2}{R_a} (1.8 - \alpha_{\text{liq}}) \\ &\quad + \frac{\Omega}{2\pi^2} \int_0^\infty S_0(q) F(q) q^2 dq, \end{aligned} \quad (26)$$

where $S_0(q)$ is the liquid structure factor,

$$S_0(q) = N \langle |S(\vec{q})|^2 \rangle, \quad (27)$$

and the effective electrostatic constant of the liquid is given by

$$\alpha_{\text{liq}} = -(2R_a/\pi) \int_0^\infty [S_0(q) - 1] dq. \quad (28)$$

In Eq. (27) the angular brackets denote a statistical average over all possible configurations of the ions. Note that the liquid structure factor is implicitly a function of both volume and temperature and therein derives the temperature dependence of $E_{\text{struc}}^{\text{liq}}$ and $E_{\text{bind}}^{\text{liq}}$.

Calculation of A_{liq} requires specific forms for both $S_0(q)$ and S_{exc} . These are, in general, unknown functionals of the true interatomic pair potential between ions,

$$v_{\text{pair}}(r) = \frac{(Z^*e)^2}{r} + \frac{\Omega}{\pi^2} \int_0^\infty F(q) \frac{\sin(qr)}{qr} q^2 dq. \quad (29)$$

In practice, however, it is only the short-range repulsive part of v_{pair} which significantly affects these quantities, so that an approximate treatment is possible. A very effective procedure is to apply so-called fluid variational theory, in which one calculates $S_0(q)$ and S_{exc} for a closely related reference fluid where the relationship to v_{pair} is known. The reference system normally contains a single variational parameter which is chosen to minimize A_{liq} when the resulting $S_0(q)$ and S_{exc} are used in Eq. (22) for the real system. According to the rigorous Gibbs-Bogolyubov inequality,⁴ this produces the closest upper-bound estimate of A_{liq} possible for this reference system. Furthermore, it follows that the "best" reference system

at a given volume and temperature is that which produces the lowest overall value of A_{liq} .

There are currently three reference systems which are available for implementing fluid variational theory. The first and most widely used is the hard-sphere (HS) fluid,⁴ in which the pair potential is assumed to be infinitely repulsive between $r=0$ and $r=\sigma$ and zero beyond. The variational parameter is the hard-sphere diameter σ , or, equivalently, the packing fraction

$$\eta = \frac{1}{6} \pi (\sigma^3 / \Omega). \quad (30)$$

The HS fluid has the desirable property that $S_0(q)$, α_{liq} , and S_{exc} can all be obtained as analytic functions of η . The latter two quantities are given by

$$\alpha_{\text{liq}}^{\text{HS}} = 6\eta^{2/3} \left[\frac{1 - \eta/5 + \eta^2/10}{1 + 2\eta} \right] \quad (31)$$

and

$$S_{\text{exc}}^{\text{HS}} = -k_B \frac{4\eta - 3\eta^2}{(1 - \eta)^2}. \quad (32)$$

In addition, the measured liquid structure factor in most metals is well represented by $S_0^{\text{HS}}(q)$ for reasonable values of η . Near the zero-pressure melting point of Al, for example, $\eta=0.44$ gives an excellent fit to the experimental structure factor for $q < 5k_F$.¹⁴

At the opposite extreme is the one-component-plasma (OCP) reference system, in which v_{pair} is the relatively soft Coulomb-type potential between point ions of charge Z_0e in a compensating uniform background. The variational quantity is Z_0 or equivalently the plasma parameter

$$\Gamma_0 = (Z_0e)^2 / R_a k_B T. \quad (33)$$

The OCP fluid has been extensively studied by Monte Carlo simulation and very accurate results now exist^{22,23} for both the total internal energy and the Helmholtz free energy of this system over a wide range of Γ_0 . These results, in turn, have been carefully fitted to analytic forms. From the most recent results of Slattery *et al.*,²³ one has

$$\alpha_{\text{liq}}^{\text{OCP}} = -\frac{2}{\Gamma_0} (a\Gamma_0 + b\Gamma_0^{1/4} + c\Gamma_0^{-1/4} + d) \quad (34)$$

and

$$S_{\text{exc}}^{\text{OCP}} = -k_B \{ 3b\Gamma_0^{1/4} - 5c\Gamma_0^{-1/4} + d(\ln\Gamma_0 - 1) - [a + 4(b - c)] - 0.436 \}, \quad (35)$$

where $a = -0.897744$, $b = 0.95043$, $c = 0.18956$, and $d = -0.81487$. The corresponding structure factor $S_0^{\text{OCP}}(q)$ does not have an analytic representation, but very recently a useful table of this function has been constructed²⁴ from solutions of the hypernetted-chain integral equation with a bridge-graph correction.²⁵ These results are in excellent agreement with Monte Carlo calculations and have the added advantage of smoothness as a function of both Γ_0 and q .

The short-range repulsive nature of real interatomic potentials in simple metals is usually intermediate between the HS and OCP limits. Figure 1 shows, for example, our

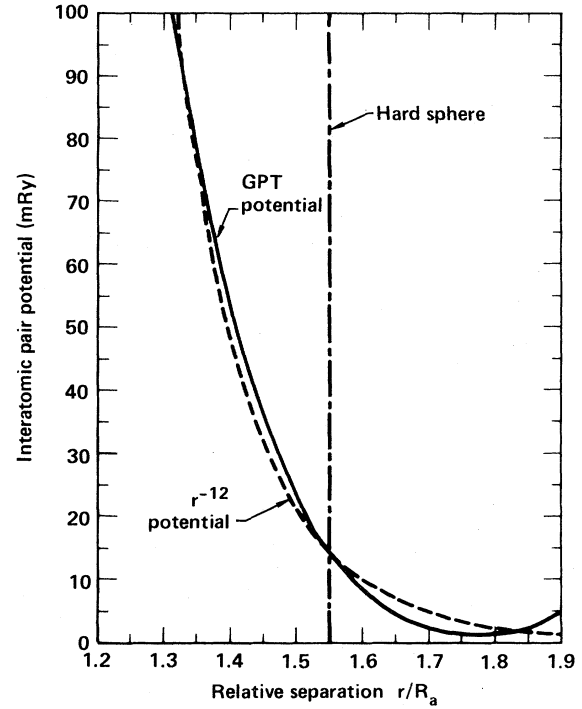


FIG. 1. Short-range repulsive portion of the GPT interatomic pair potential in Al, as calculated from Eq. (29) at $\Omega=128.0$ a.u. Shown for comparison is the corresponding hard-sphere diameter σ obtained from fluid variational theory and a fitted r^{-12} potential.

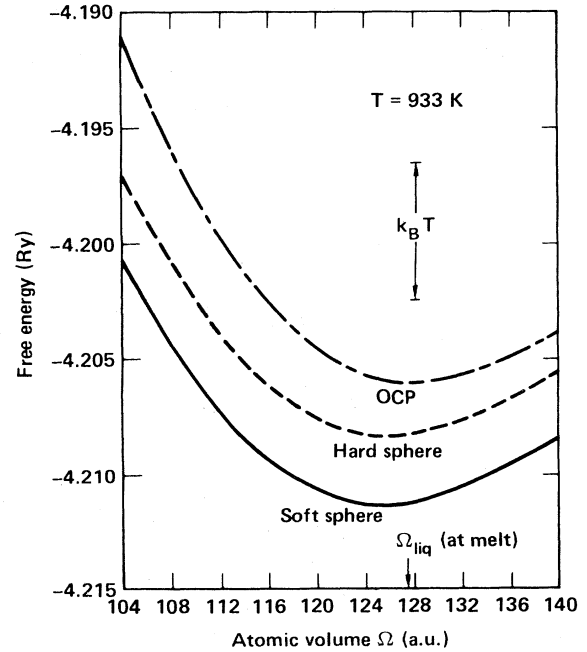


FIG. 2. GPT liquid free energy $A_{\text{liq}}(\Omega, T)$ versus volume near normal melting conditions in Al, as calculated for the one-component-plasma (OCP), hard-sphere, and soft-sphere reference systems. The observed liquid volume Ω_{liq} at melt is indicated.

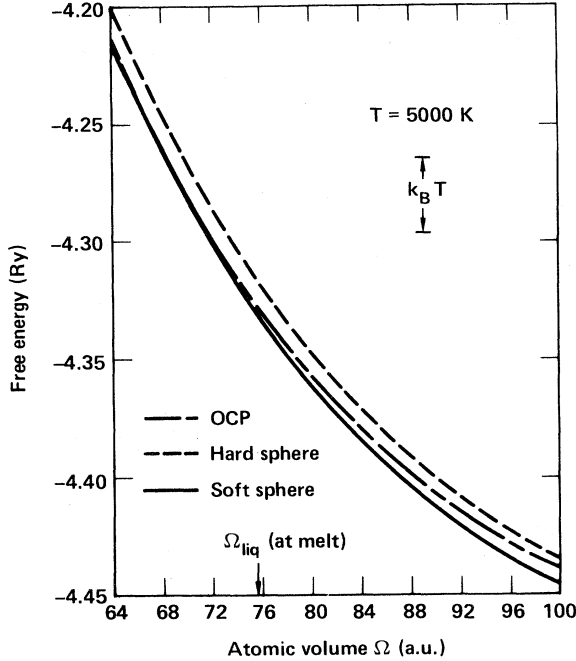


FIG. 3. GPT liquid free energy $A_{\text{liq}}(\Omega, T)$ versus volume near representative high-pressure melting conditions in Al, as calculated for the one-component-plasma (OCP), hard-sphere, and soft-sphere reference systems. The calculated liquid volume Ω_{liq} at melt is indicated.

first-principles GPT pair potential for Al near the normal liquid density. In the critical region around $r = \sigma$, this potential varies roughly as r^{-12} . A reference system which better accommodates this behavior is the so-called soft-sphere (SS) model of Ross.¹² In the SS fluid, the HS packing fraction η is retained as the variational parameter and the form of the structure factor $S_0^{\text{HS}}(q)$ is taken over directly. The entropy function, however, is modified to simulate the free energy of the softer r^{-12} potential, as determined by Monte Carlo calculations. This leads to

$$S_{\text{exc}}^{\text{SS}} = -k_B \left[\frac{4\eta - 3\eta^2}{(1-\eta)^2} - (\eta^4/2 + \eta^2 + \eta/2) \right]. \quad (36)$$

Thus the SS reference system retains all of the desirable features of the HS system, while at the same time producing a lower and hence more accurate free energy in a metal like Al.

We have performed GPT calculations of A_{liq} as a function of volume and temperature in Al using all three liquid reference systems, and we indeed find that the SS model always produces the lowest free energy. Representative results in the vicinity of melting are illustrated in Figs. 2 and 3. As shown in Fig. 2, the spread in free energies among the three reference systems around normal melting conditions is on the order of $k_B T_m$, where $T_m = 933$ K is the experimental melting temperature, with the OCP system producing the highest free energy. At the zero-pressure liquid density ($\Omega = 127.0$ a.u.), our result for the OCP–HS energy difference is also in qualitative agreement with that previously obtained by Mon

et al.^{14,26} for Al using a parametrized local pseudopotential. At higher densities and temperatures, on the other hand, the relative spread of free energies decreases, with the OCP free energy dropping below that of the HS system and closely approaching (although never crossing below) the SS value, as shown in Fig. 3.

C. HLP parameters and application

The four free parameters of our HLP model have been determined by fitting to solid-phase thermodynamic data. The parameters r_c and β in the core pseudopotential were established by first requiring that the total internal pressure

$$P_{\text{sol}}(\Omega, T) = - \frac{\partial A_{\text{sol}}(\Omega, T)}{\partial \Omega}, \quad (37)$$

both vanish at the observed room-temperature equilibrium density ($\Omega = \Omega_0 = 112.0$ a.u.) and match an accurate first-principles augmented-plane-wave (APW) energy-band calculation²⁷ of the $T=0$ isotherm at high compression. The remaining exchange-correlation parameters α and ξ were then chosen to simultaneously reproduce the observed normal-density Grüneisen parameter [$\gamma_G(\Omega_0) \sim 2.1$],²⁸ calculated here as

$$\gamma_G(\Omega) = - \frac{1}{3N} \sum_{\vec{q}, \lambda} \frac{\partial \ln \nu_{\lambda}(\vec{q})}{\partial \ln \Omega}, \quad (38)$$

as well as experimental isotherms to 100 kbar at 300 (Ref. 29) and 673 K (Ref. 30). This fitting procedure gave values of $\beta = 50$ Ry a.u.³, $r_c = 0.3015$ a.u., and $\alpha = \xi = 0.625$.

In applying the HLP model, an additional volume-dependent term,

$$A_{\text{el}}(\Omega, T) = -Z \left[\frac{\pi}{2} \right]^2 \frac{(k_B T)^2}{\epsilon_F}, \quad (39)$$

for the thermal free energy of the valence electrons, has also been added to both A_{sol} and A_{liq} . This correction has a negligible effect on both the low-temperature thermodynamic properties and the melting-curve calculation in Al, but it does significantly affect the calculated Hugoniot temperature at high pressure and has, therefore, been retained. All of the GPT calculations reported here, on the other hand, have been performed with this term omitted.

Before finally turning to the melting calculation in Al, it is of interest to briefly discuss GPT predictions of those physical quantities which have been fitted in our HLP model. The GPT gives a room-temperature equilibrium atomic volume of $\Omega = 116.2$ a.u., which is about 4% above the experimental value. The calculated pressure in the solid, P_{sol} , is consequently overestimated somewhat at any given volume. This is illustrated in Fig. 4, where HLP and GPT $T=300$ K isotherms are compared. At $\Omega = 68$ a.u. ($\Omega/\Omega_0 = 0.607$), approximately the smallest solid volume considered in our GPT melting calculation, we estimate that P_{sol} at $T=0$ is too large by about 150 kbar relative to the theoretical APW result. This amounts to about 10% of the total GPT-calculated pressure at

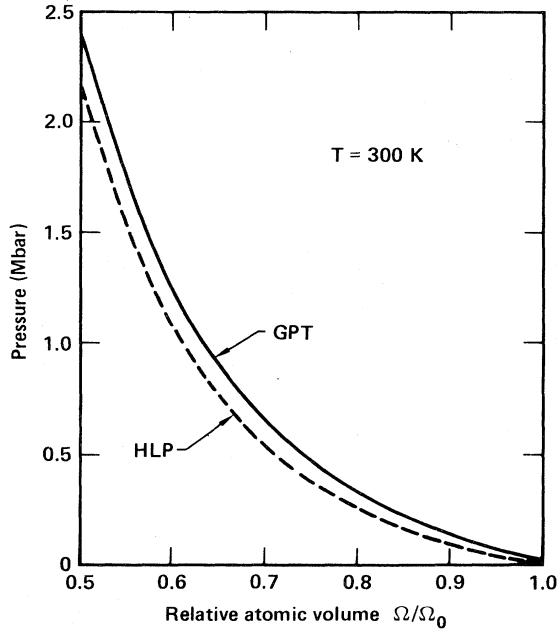


FIG. 4. Comparison of the calculated HLP and GPT $T=300$ K isotherms over the volume range from normal solid density ($\Omega = \Omega_0 = 112.0$ a.u.) to twofold compression.

melting. Finally, the computed GPT value of $\gamma_G(\Omega_0)$ is 1.9, approximately 10% below the experimental value. Under compression, the HLP and GPT $\gamma_G(\Omega)$ curves move closer together with the former just crossing below the latter near $\Omega/\Omega_0 = 0.6$, as shown in Fig. 5. Thus for

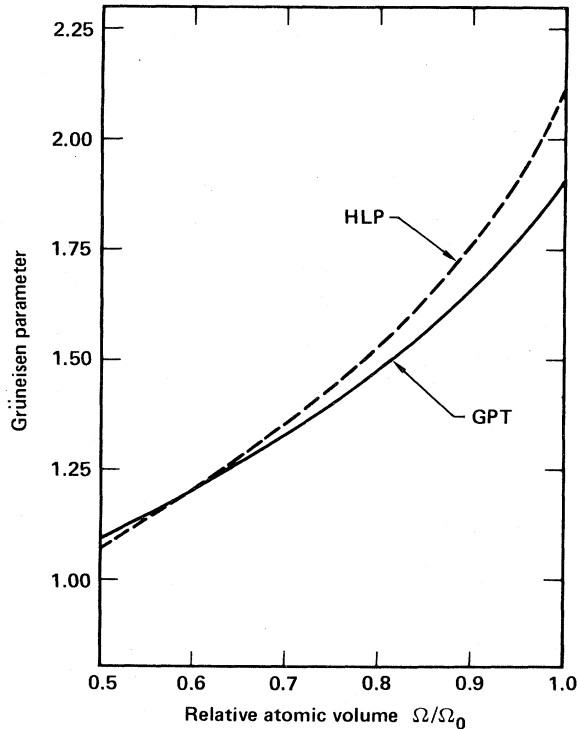


FIG. 5. Comparison of the calculated HLP and GPT Grüneisen parameters [$\gamma_G(\Omega)$] as a function of volume in the solid over the same range as in Fig. 4.

all of the basic solid-phase thermodynamic properties of Al of relevance here, the HLP and GPT results agree with each other and with experiment to 10% or better.

IV. MELTING CURVE

In general, the melting curve $P_m(T_m)$ is established by equating solid and liquid Gibbs free energies as a function of pressure and temperature:

$$G_{\text{sol}}(P_m, T_m) = G_{\text{liq}}(P_m, T_m). \quad (40)$$

In practice, however, it is often a difficult task to apply Eq. (40) directly because it necessitates finding the intersection of two nearly parallel curves. Fortunately, there are simple alternate procedures available. At low pressure, one may use the equivalent common tangent construction on the respective Helmholtz-free-energy-versus-volume curves at fixed temperature $T = T_m$ to find the corresponding melting pressure P_m . At higher pressure, one can proceed by first finding the volume of intersection Ω_{av} of $A_{\text{sol}}(\Omega, T_m)$ and $A_{\text{liq}}(\Omega, T_m)$. This will always be intermediate between the true solid and liquid volumes at melting:

$$\Omega_{\text{sol}} < \Omega_{\text{av}} < \Omega_{\text{liq}}. \quad (41)$$

If the change in volume,

$$\Delta\Omega = \Omega_{\text{liq}} - \Omega_{\text{sol}}, \quad (42)$$

is small, little error is incurred by assuming

$$P_m = \frac{1}{2} [P_{\text{sol}}(\Omega_{\text{av}}, T_m) + P_{\text{liq}}(\Omega_{\text{av}}, T_m)], \quad (43)$$

with P_{sol} calculated from Eq. (37) and P_{liq} from the corresponding expression in the liquid. The same pressure-volume relations may be further used to obtain Ω_{sol} and Ω_{liq} from a knowledge of P_m . In the case of Al, $\Delta\Omega$ is always less than 5% of Ω_{av} , so that this procedure works quite well. We have confirmed this for our GPT results by using both Eqs. (40) and (43) to determine points on the high-pressure melting curve. In this regard, the latter approximate procedure is even to be preferred, since the former introduces some amount of unphysical curvature into the melting curve because of the difficulty in locating the precise intersection of the solid and liquid Gibbs free energies. Equation (43) has been used in both the GPT and HLP results presented below for $P_m \geq 80$ kbar.

Utilizing the SS liquid reference system, GPT and HLP melting curves have been calculated in the pressure range $P_m \leq 2$ Mbar. Our low-pressure GPT result is illustrated and compared with experiment³¹ in Fig. 6 over the limited range where present data exists (to ~ 60 kbar). Corresponding zero-pressure melting properties are listed in Table I. The calculated properties include the latent heat of fusion, given at $P_m = 0$ by

$$\begin{aligned} L &= E_{\text{bind}}^{\text{liq}}(\Omega_{\text{liq}}, T_m) + E_{\text{gas}}(T_m) \\ &\quad - E_{\text{bind}}^{\text{sol}}(\Omega_{\text{sol}}) - E_{\text{ph}}(\Omega_{\text{sol}}, T_m) \\ &\approx E_{\text{bind}}^{\text{liq}}(\Omega_{\text{liq}}, T_m) - E_{\text{bind}}^{\text{sol}}(\Omega_{\text{sol}}) - \frac{3}{2} k_B T_m, \end{aligned} \quad (44)$$

where $E_{\text{ph}} \approx 3k_B T_m$, the increase in entropy upon melting,

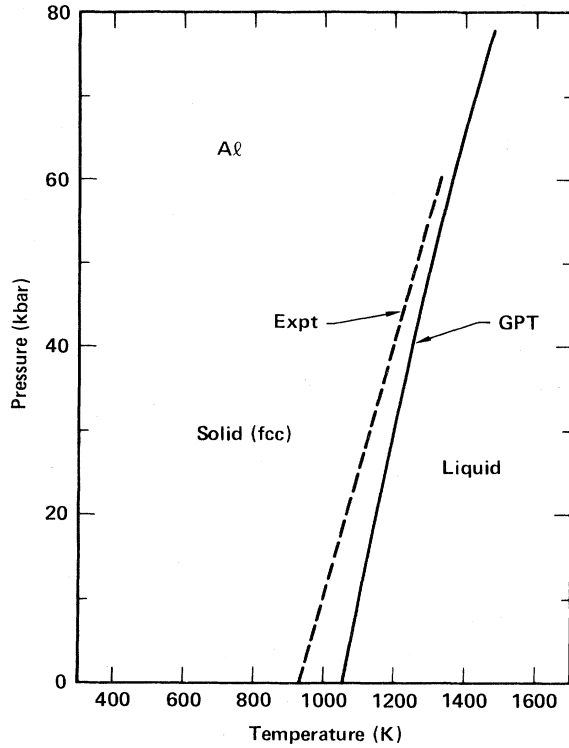


FIG. 6. Theoretical GPT melting curve versus experiment (Ref. 31) in Al over the limited pressure range where the latter data is available for comparison.

$$\begin{aligned} \Delta S &= S_{\text{exc}}(\Omega_{\text{liq}}, T_m) + S_{\text{gas}}(\Omega_{\text{liq}}, T_m) - S_{\text{ph}}(\Omega_{\text{sol}}, T_m) \\ &= L/T_m, \end{aligned} \quad (45)$$

and the Clausius-Clapeyron value of the initial slope of the melting curve,

$$\frac{dP_m}{dT_m} = \frac{L}{T_m \Delta\Omega}. \quad (46)$$

The overall agreement with experiment displayed in Fig. 6 and Table I seems quite satisfactory, especially considering our neglect of anharmonic effects in the solid. The

importance of the liquid reference system to this general success is most pronounced in the melting temperature itself. If the SS system is replaced by the HS one, for instance, the computed value of T_m at zero pressure rises from 1050 to 1800 K. With the SS reference system, the largest independent error is the 35% underestimate of $\Delta\Omega$, although, by the same token, this quantity is percentage-wise more uncertainly determined than Ω_{liq} , Ω_{sol} , or T_m . The reason is that at $P_m=0$, $\Delta\Omega$ depends rather sensitively on the precise location of the minima in the Helmholtz free energies $A_{\text{liq}}(\Omega, T_m)$ and $A_{\text{sol}}(\Omega, T_m)$. Errors on the order of only 1% in determining Ω_{liq} and/or Ω_{sol} , for example, could account for the entire 35% underestimate, while at the same time having little effect on T_m . In any case, the corresponding low values obtained for L and ΔS in Table I directly reflect the underestimate in $\Delta\Omega$. This is clear from the excellent calculated value of dP_m/dT_m using Eq. (46), where the dependence of L on $\Delta\Omega$ approximately cancels out on the right-hand side of that equation. Our dP_m/dT_m result is also in good agreement with the theoretical melting-curve slope obtained in Fig. 6.

We were unfortunately not able to obtain corresponding HLP results near zero pressure because some of the calculated phonon frequencies were found to be imaginary at expanded volumes. Since the GPT-calculated phonons showed no such tendency, even at 30% expansion, we expect that this is an artifact of the HLP model, possibly related to the choice of parameters. In this regard, we note that the fitted value of α in Eq. (18) for $G(q)$ is too large by about a factor of 2 relative to that given by electron-gas theory [i.e., Eq. (11)], tending to overly depress the calculated phonon frequencies at small q . Moreover, Jones,⁵ using the same model with a theoretical $G(q)$ closer to Eq. (11) at small q , found no such anomaly. Our primary motivation for introducing the semiempirical form (18) for $G(q)$ in the HLP model was to obtain a more realistic Grüneisen parameter $\gamma_G(\Omega)$ (Fig. 5) than could be otherwise achieved. While this may have resulted in some adverse effects on the low- q phonons, the higher- q phonons, which are those which dominate thermodynamic properties, are not so affected. This is demonstrated in Fig. 7, where the HLP and GPT values

TABLE I. Calculated GPT melting properties in Al at zero pressure compared with experiment. Included are the melting temperature T_m , atomic volumes Ω_{sol} , Ω_{liq} , and $\Delta\Omega$, latent heat of fusion L , entropies ΔS and $-S_{\text{exc}}$, and initial slope of the melting curve dP_m/dT_m obtained from the Clausius-Clapeyron equation (46).

	T_m (K)	Ω_{sol} (a.u.)	Ω_{liq} (a.u.)	$\Delta\Omega$ (a.u.)	L (mRy/atom)	ΔS (k_B)	$-S_{\text{exc}}$ (k_B)	dP_m/dT_m (kbar/K)
Theory	1050	122.2	126.4	4.2	6.11	0.92	4.0	0.20
Experiment	933	120.5 ^a	127.0 ^{a,b}	6.5 ^a	8.25 ^c 8.0 ^d	1.39 ^e 1.34 ^d	3.6 ^e	0.20 ^f 0.19 ^g

^aReference 32.

^bReference 33.

^cReference 7.

^dReference 34, p. 381.

^eReference 35, p. 80.

^fWith $L=8.25$, $\Delta\Omega=6.5$, and $T_m=933$.

^gWith $L=8.0$, $\Delta\Omega=6.5$, and $T_m=933$.

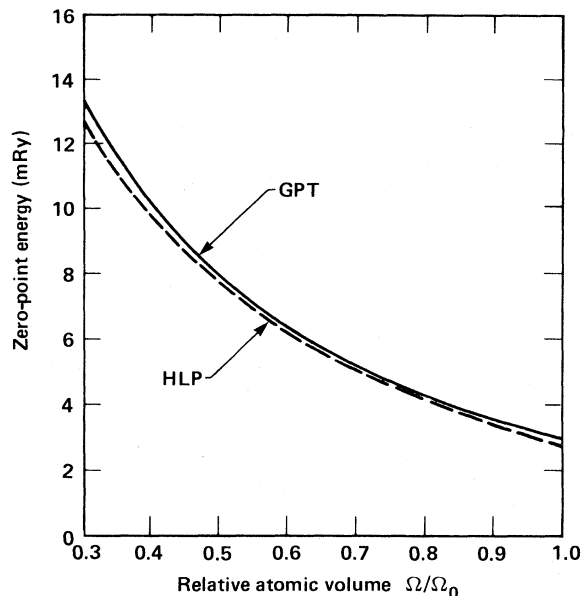


FIG. 7. Comparison of the calculated HLP and GPT zero-point vibrational energies [$E_{\text{ph}}^0(\Omega)$] as a function of volume in the solid.

of the zero-point vibrational energy, $E_{\text{ph}}^0(\Omega) \equiv E_{\text{ph}}(\Omega, 0)$, given by

$$E_{\text{ph}}^0(\Omega) = \frac{1}{2N} \sum_{\vec{q}, \lambda} h\nu_{\lambda}(\vec{q}), \quad (47)$$

are compared as a function of volume. The agreement is seen to be uniformly excellent.

At smaller melting volumes, our HLP model is entirely well behaved and we were able to obtain a meaningful melting curve in the pressure range $P_m \geq 96$ kbar, corresponding to $T_m \geq 1500$ K. This result is illustrated in Fig. 8 and compared there with the corresponding GPT melting curve. The two theories agree remarkably well considering the nontrivial difference in the details of the approaches. Nonetheless, at the higher pressures the HLP and GPT melting curves do begin to diverge significantly. At $T_m = 6000$ K, this amounts to a difference in calculated P_m of 430 kbar. The origin of this divergence is possibly related to the effects of pseudopotential nonlocality on the structural energies. In this regard, neither the direct

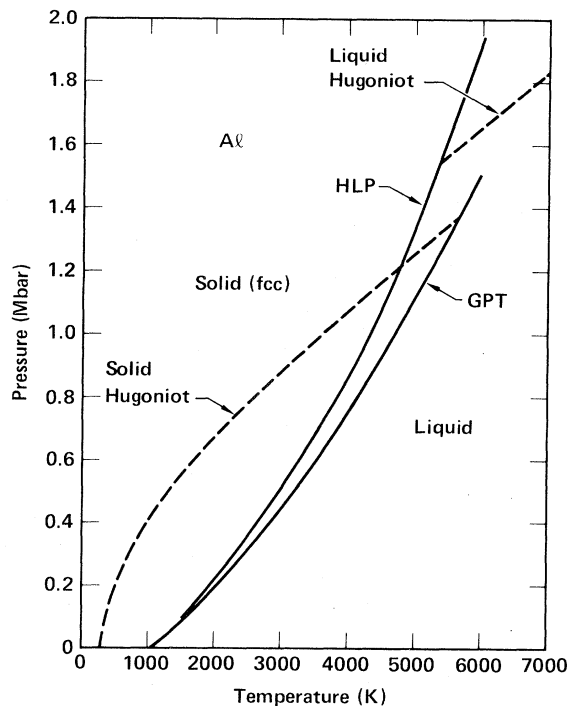


FIG. 8. Comparison of the theoretical HLP and GPT melting curves (solid lines) in Al over the full temperature and pressure ranges considered in this work. Also shown is the predicted melting on the shock Hugoniot of Al, as obtained from HLP calculations of the solid and liquid Hugoniot (dashed lines).

differences between the HLP and GPT pressure-volume relations (e.g, Fig. 4) nor the d -state hybridization included in the GPT account for this behavior. At $T_m = 6000$ K, the latter two effects respectively raise the GPT melting pressure by 150 kbar and lower it by 40 kbar, so that their combined impact is actually to improve the agreement with the HLP result. On the other hand, it is also quite possible that the divergence would be lessened if the GPT pseudopotentials were adjusted to reproduce all of the same EOS data fitted in the HLP model.

Calculated properties along the GPT and HLP melting curves are given in Tables II and III, respectively. In both treatments, the packing fraction η is found to remain approximately constant, and at similar values, decreasing

TABLE II. Calculated properties along the GPT melting curve in Al. Included are the melting temperature T_m , pressure P_m , atomic volumes Ω_{av} , Ω_{sol} , and Ω_{liq} , fractional volume increase upon melting $\Delta\Omega/\Omega_{\text{sol}}$, liquid packing fraction η , and Lindemann ratio α_{Lind} .

T_m (K)	P_m (Mbar)	Ω_{av} (a.u.)	Ω_{sol} (a.u.)	Ω_{liq} (a.u.)	$\Delta\Omega/\Omega_{\text{sol}}$	η	α_{Lind}
1050	0.0	124.5	122.2	126.4	0.034	0.48	0.23
1500	0.080	114.4	111.9	116.8	0.044	0.47	0.24
2000	0.187	105.4	103.4	107.3	0.038	0.46	0.24
3000	0.443	91.9	90.1	93.5	0.039	0.46	0.25
4000	0.752	82.0	80.7	83.3	0.032	0.46	0.25
5000	1.12	74.5	73.2	75.7	0.033	0.45	0.26
6000	1.51	68.4	67.4	69.6	0.033	0.45	0.26

TABLE III. Calculated properties along the HLP melting curve in Al. Notation and units are the same as in Table II.

T_m (K)	P_m (Mbar)	Ω_{av} (a.u.)	Ω_{sol} (a.u.)	Ω_{liq} (a.u.)	$\Delta\Omega/\Omega_{sol}$	η	x_{Lind}
1500	0.096	109.3	106.8	111.8	0.047	0.47	0.23
2000	0.211	99.7	97.7	101.8	0.042	0.47	0.23
3000	0.506	85.5	84.0	87.0	0.036	0.47	0.23
4000	0.876	75.6	74.5	76.8	0.031	0.47	0.24
5000	1.35	67.7	66.8	68.6	0.027	0.46	0.24
6000	1.94	61.3	60.5	62.1	0.026	0.46	0.24

only slightly with compression. The Lindemann ratio in the solid,

$$x_{Lind} = \frac{3\hbar}{\Theta_D R_a} \left[\frac{T_m}{k_B M} \right]^{1/2}, \quad (48)$$

also remains fairly constant, increasing slowly with compression. Note, however, that both the GPT and HLP results predict a more rapid rise of T_m with increasing pressure than does a Lindemann law with constant x_{Lind} . In obtaining x_{Lind} here, the Debye temperature Θ_D in Eq. (48) has been inferred from the calculated zero-point vibrational energy by the Debye formula $E_{ph}^0(\Omega) = \frac{9}{8} k_B \Theta_D$. At normal solid density, the GPT and HLP values of Θ_D so obtained are 420 and 397 K, respectively, in good agreement with the experimental value of 394 K.

Another slowly varying quantity along the melting curve is the fractional volume change upon melting, $\Delta\Omega/\Omega_{sol}$, as also listed in Tables II and III. This quantity initially tends to decrease slightly with increasing pressure, before leveling off at very high pressure. The same general magnitudes of $\Delta\Omega/\Omega_{sol}$ are obtained in the GPT and HLP treatments, although the former values show some slight, probably unphysical, fluctuations, in addition to the low value at $P_m=0$ already noted above. These fluctuations are likely an artifact of small quantitative errors in the determination of $\Delta\Omega$, possibly arising from the numerical differentiation used to obtain pressures in the GPT. Also in this regard, the low GPT value of $\Delta\Omega/\Omega_{sol}$ at $P_m=0$ is clearly out of sequence with the higher-pressure values. It is interesting to note that, in contrast, the experimental value of $\Delta\Omega/\Omega_{sol}=0.054$ at $P_m=0$ fits both the GPT and HLP high-pressure sequences very well.

Finally, our HLP model has been used to determine solid and liquid Hugoniot in Al. These have been calculated from an assumed starting state of $P=0$, $\Omega=112.0$ a.u., and $T=300$ K, reflecting the normal experimental conditions. The intersection of the Hugoniot with the HLP melting curve is illustrated in Fig. 8. From this result we infer that melting on the actual shock Hugoniot should begin at about $P_m=1.2$ Mbar and end at about $P_m=1.55$ Mbar, in agreement with McQueen's recent preliminary experimental measurements of 1.25 and 1.5 Mbar, respectively.¹⁶ We have not attempted a compar-

able GPT calculation, partly because the corresponding theoretical Hugoniot will not, of course, match the precise experimental starting conditions without adjustment. If, however, one simply extrapolates the HLP solid Hugoniot to the GPT melting curve, as is done in Fig. 8, an initial melting pressure of approximately 1.4 Mbar is inferred, so that no large difference in the theoretical prediction is expected in any case.

V. CONCLUSIONS

The general overall agreement obtained for the melting properties of Al both between theory and experiment and between the distinct HLP and GPT theoretical treatments themselves is very encouraging. Apart from uncertainties about anharmonicity in the solid at low pressure, the combination of pseudopotential perturbation theory, lattice dynamics in the harmonic approximation for the solid, and fluid variational theory with suitable reference system for the liquid indeed seems capable of giving accurate results over a wide range of pressure in this metal. In particular, we have clearly identified the soft-sphere reference system in fluid variational theory as not only being the best such system available for the case of Al, but also as quite essential to the quantitative success we have achieved. There is also considerable support for the general premise of our HLP study, namely, that a local pseudopotential accurately fit to EOS data can be successfully transferred to the calculation of the melting curve. On the other hand, the differences between the HLP and GPT melting curves at high pressure should not be regarded as negligible either, so that pseudopotential nonlocality is apparently significant. This latter aspect of the problem needs further clarification, however. One interesting possibility for the future in this regard is to fine tune the non-local GPT pseudopotentials to the same EOS data and then reexamine the melting curve.

ACKNOWLEDGMENTS

The authors wish to thank Dr. R. G. McQueen for kindly providing his available experimental results on shock-Hugoniot melting in Al. This work was performed, under the auspices of the U. S. Department of Energy, by Lawrence Livermore National Laboratory under Contract No. W-7405-Eng-48.

- ¹D. Stroud and N. W. Ashcroft, *Phys. Rev. B* **5**, 371 (1972).
- ²W. A. Harrison, *Pseudopotentials in the Theory of Metals* (Benjamin, New York, 1966).
- ³V. Heine and D. Weaire, in *Solid State Physics*, edited by F. Seitz, D. Turnbull, and H. Ehrenreich (Academic, New York, 1970), Vol. 24, p. 249.
- ⁴N. W. Ashcroft and D. Stroud, in *Solid State Physics*, edited by F. Seitz, D. Turnbull, and H. Ehrenreich (Academic, New York, 1978), Vol. 33, p. 1, and references therein.
- ⁵H. D. Jones, *Phys. Rev. A* **8**, 3215 (1973).
- ⁶D. A. Young and M. Ross, *Phys. Rev. B* **29**, 682 (1984).
- ⁷W. M. Hartmann, *Phys. Rev. Lett.* **26**, 1640 (1971).
- ⁸J. A. Moriarty, *Phys. Rev. B* **26**, 1754 (1982); **16**, 2537 (1977).
- ⁹A. K. McMahan and J. A. Moriarty, *Phys. Rev. B* **27**, 3235 (1983).
- ¹⁰G. K. Straub, R. E. Swanson, B. L. Holian, and D. C. Wallace, in *Ab Initio Calculation of Phonon Spectra*, edited by J. T. Devreese, V. E. Van Doren, and P. E. Van Camp (Plenum, New York, 1983), p. 137; R. E. Swanson, G. K. Straub, B. L. Holian, and D. C. Wallace, *Phys. Rev. B* **25**, 7807 (1982); B. L. Holian, G. K. Straub, R. E. Swanson, and D. C. Wallace, *ibid.* **27**, 2873 (1983).
- ¹¹E.g., E. R. Cowley and R. C. Shukla, *Phys. Rev. B* **9**, 1261 (1974).
- ¹²M. Ross, *J. Chem. Phys.* **71**, 1567 (1979).
- ¹³M. Ross, H. E. DeWitt, and W. B. Hubbard, *Phys. Rev. A* **24**, 1016 (1981).
- ¹⁴K. K. Mon, R. Gann, and D. Stroud, *Phys. Rev. A* **24**, 2145 (1981).
- ¹⁵J. M. Brown and R. G. McQueen, in *Advances in Earth and Planetary Sciences: High-Pressure Research in Geophysics*, edited by S. Akimoto and M. H. Manghnani (Center for Academic Publications Japan, Tokyo, 1982), Vol. 12, p. 611.
- ¹⁶R. G. McQueen (private communication); J. W. Shaner, J. M. Brown, and R. G. McQueen, in *Proceedings of the Ninth AIRAPT International High-Pressure Conference* (1983) (in press). These preliminary measurements were made on 2024 Al, a dilute alloy containing 93% Al by weight. Additional measurements on pure Al are in progress, but only small changes in the results are expected.
- ¹⁷W. Kohn and L. J. Sham, *Phys. Rev.* **140**, A1133 (1965).
- ¹⁸For a recent review, see K. S. Singwi and M. P. Tosi, in *Solid State Physics*, edited by F. Seitz, D. Turnbull, and H. Ehrenreich (Academic, New York, 1981), Vol. 36, p. 177.
- ¹⁹D. J. W. Geldart and R. Taylor, *Can. J. Phys.* **48**, 167 (1970).
- ²⁰L. Hedin and B. I. Lundqvist, *J. Phys. C* **4**, 2064 (1971).
- ²¹J. A. Moriarty, *Phys. Rev. B* **8**, 1338 (1973).
- ²²W. L. Slattery, G. D. Doolen, and H. E. DeWitt, *Phys. Rev. A* **21**, 2087 (1980).
- ²³W. L. Slattery, G. D. Doolen, and H. E. DeWitt, *Phys. Rev. A* **26**, 2255 (1982).
- ²⁴F. J. Rogers, D. A. Young, H. E. DeWitt, and M. Ross, *Phys. Rev. A* **28**, 2990 (1983).
- ²⁵Y. Rosenfeld and N. W. Ashcroft, *Phys. Rev. A* **20**, 1208 (1979).
- ²⁶The OCP results of Mon *et al.* (Ref. 14), however, appear to have quantitatively suffered from the use of the OCP parameters listed in Ref. 22, where the entropy constant is incorrectly given as 0.420 instead of 0.436. Mon *et al.* calculated $\Gamma_0=255$ (well above the OCP freezing value) for liquid Al, whereas we obtain $\Gamma_0=140$ at the same density and temperature.
- ²⁷A. K. McMahan and M. Ross, in *High-Pressure Science and Technology*, edited by K. D. Timmerhaus and M. S. Barber (Plenum, New York, 1979), Vol. 2, p. 920.
- ²⁸K. A. Gschneider, in *Solid State Physics*, edited by F. Seitz, D. Turnbull, and H. Ehrenreich (Academic, New York, 1964), Vol. 16, p. 275.
- ²⁹K. Syassen and W. B. Holzapfel, *J. Appl. Phys.* **49**, 4427 (1978).
- ³⁰L. M. Lityagina, Z. V. Malyushitskaya, T. A. Pashkina, and S. S. Kabalkina, *Phys. Status Solidi A* **69**, K147 (1982).
- ³¹J. Lees and B. H. J. Williamson, *Nature* **208**, 278 (1965).
- ³²S. P. Kazachkov, N. M. Kochegura, and E. A. Markovskiy, *Russ. Metall.* **1/1979**, 65 (1979).
- ³³D. J. Steinberg, *Trans. Metall. Soc. AIME* **5**, 1341 (1974).
- ³⁴M. Shimoji, *Liquid Metals* (Academic, New York, 1977).
- ³⁵T. E. Faber, *An Introduction to the Theory of Liquid Metals* (Cambridge, London, 1972).